CONF-910580--1

DE91 015274

DYNAMICS OF LATTICE DAMAGE ACCUMULATION FOR MeV IONS IN SILICON

A.GOLANSKI*, A.GROB**, J.J.GROB**, O.W.HOLLAND***, S.J.PENNYCOOK*** and C.W.WHITE***

* Centre National d'Etudes des Telecommunications, B.P.98 38240 Meylan, France.

** Centre de Recherches Nucleaires, Laboratoire "PHASE", B.P.20, 67037 Strasbourg, France.

***Oak Ridge National Laboratory, Oak Ridge, TN.37831, USA

ABSTRACT

Although the domination of electronic stopping over nuclear stopping may be regarded as an important practical advantage for high energy (MeV) ion processing, exact knowledge of the doping introduced into the active regions as well as of the process-associated defects and their thermal stability is essential for an understanding of device performance. In the present work we review the results of our recent investigations into lattice damage accumulation in single crystal Si resulting from high energy ion implantation in the implantation temperature (T_i) range between liquid nitrogen temperature and 200°C. The ion species used were 1 MeV O^+, 1.25 MeV Si^+ and 4.8 MeV Er^+ ($0.2<M_2/M_1<1.7$). Ion implantation was carried out using virgin Si as well as Si containing pre-existintg damage. The lattice damage was studied using Rutherford backscattering/channeling spectrometry (RBS) and cross-sectional transmission electron microscopy (XTEM). The experimental results are correlated with the predictions of the model of Hecking and Te Kaat (Appl.Surf.Sc.43, 87, 1989). The temperature dependence of the damage accumulation in the virgin Si suggests that the annihilation of simple defects via intra-cascade and inter-cascade recombination processes is controlled mainly by the T, while the nucleation of defect clusters during implantation appears to be influenced by spatial proximity effects related to the deposited energy density. Finally, the dynamics of damage accumulation is shown to be strongly influenced by the pre-existing damage structure.

(Research sponsored by the Division of Materials Sciences, U.S. Department of Energy under contract DE-AC05-84OR21400 with Martin Marietta Energy Systems, Inc.).

DISCLAIMER

INTRODUCTION

Ion induced radiation damage in silicon has been extensively studied over the last twenty years [see ref.1 and references therein]. Most of the investigations have focused on the energy range between several tens of keV to about 200 keV, a range which corresponds to well established industrial applications. Recently, the trend towards increased density in VLSI circuits and the maturity in the design of high energy implanters have created a new situation in which technological applications of the MeV energy range are becoming increasingly important. Process applications for MeV ion implantation fall into several classes ([1] and ref. therein):

- formation of deep (>2 μm) junctions (deep wells for CMOS devices, buried grid structures for reduction of soft errors in memory devices). In comparison with the conventional production technique (pre-deposition and drive-in), high energy implantation allows reduction in the thermal budget by a factor of about 10. It also allows the lateral diffusion of the dopant to be reduced and the integration density to be increased;
- customization of memory cells by adjustment of threshold voltages or adjustment of resistor values via implantation through the existing overlays late in the process cycle (late-process programming of memory cells for ROMs and custom microprocessors). This allows for considerable

improvement in the flexibility of the fabrication process and its adjustment to the current needs of the market;

- formation of buried damaged layers for impurity gettering;

For the MeV ion energy electronic stopping dominates over nuclear stopping and the damage can therefore be expected to be localized near the end of the ion path. Although this may be turned to considerable practical advantage for high energy processing, exact knowledge of the doping introduced into the active regions as well as identification of process-associated defects and their thermal stability is essential for an understanding of device performance.

In the present work we review the results of our recent investigations into lattice damage accumulation in single crystal Si, resulting from high energy (MeV) ion implantation, in an attempt to correlate the damage morphology of the "as implanted" state with the basic parameters of the implantation process, such as target temperature and deposited energy density, as well as with the presence of the pre-existing damage.

EXPERIMENTAL

The <100> and <111> oriented single crystal Si samples were implanted using either 1 MeV O^+, 1.25 MeV Si^+ or 4.8 MeV Er^+ ions. Oxygen ions were implanted using a single-ended Van de Graaff accelerator while Si and Er beams were produced using a General Ionex tandem machine. The use of a tandem accelerator ensures that the Si beam will be free of any contaminants, such as molecular ions of the same mass-to-charge ratio. Careful precautions were taken in order to minimize channeling effects during implantation. The beam current density was varied between several nA/cm^2 for Er^+ and 0.1 $\mu A/cm^2$ for O^+ implants. The implantation temperature T_i was regulated between liquid nitrogen (LN) temperature and 200°C using a heater located within the sample holder. Implanted doses ranged from $3x10^{14}/cm^2$ to $2x10^{16}/cm^2$ for O^+, from $3x10^{14}/cm^2$ to $3x10^{15}/cm^2$ for Si^+ and from $5x10^{12}/cm^2$ to $6x10^{13}/cm^2$ for Er^+. In a double irradiation experiment samples previously implanted at room temperature using a dose of $4.5x10^{13}/cm^2$ of 4.8 MeV Er^+ were subsequently re-implanted at T_i=200°C using a dose of $6x10^{13}/cm^2$. The implanted samples were characterized using backscattering/channeling spectroscopy with 2.8 MeV He ions and cross-sectional transmission electron microscopy (XTEM).

HIGH ENERGY COLLISION CASCADE

Figure 1 shows the energy dependence of the E_ν/E_η ratio, representing the relative contribution of the elastic (E_ν) and inelastic (E_η) energy losses for the ions used (or quoted) in the present work. The maximum values of the electronic stopping dE_η/dx calculated using TRIM-Monte Carlo code [2] are close to 1×10^3 eV/nm for 1 MeV O^+ and 1.25 MeV Si^+ ions, and to 3×10^3 eV/nm for 4.8 MeV Er^+. Although these figures are an order of magnitude higher than the dE_η/dx values corresponding to the "conventional" implantation energies (30-200 keV), they are an order of magnitude lower than the electronic energy loss leading to the formation of ionization energy spikes in isolators [3]. The substrate used in the present study is a semiconductor and the primary production of point defects is expected to be dominated by the energy deposition via elastic collisions. Concepts such as the average density of energy deposited via elastic interactions ($\bar{E}_d$) or local density of primary defects ($\bar{N}_d$), as well as correlation between $\bar{E}_d$ and $\bar{N}_d$ offered an appreciable guidance in understanding the mechanisms of lattice damage accumulation for the conventional energy range [3]. Application of these concepts for the MeV energy range, athough potentialy promising, should be considerd with caution as the high energy cascades are expected to be strongly inhomogeneous since they are composed of isolated subcascades. For

energies and ions used in this work the energy transfer to knock-ons and the probability of high energy transfer are significant [4]. One might therefore expect the morphology of high energy induced damage to show little dependence on the nature of the projectile, unless the energy density related effects play an appreciable role. The M_2/M_1 ratios corresponding to the ions used in this work (as well as in the ref.[5]) are shown in Table I. The minimum and maximum M_2/M_1 values differ by an order of magnitude, suggesting that the corresponding $\bar{E}_d$ and $\bar{N}_d$ values might be significantly different. In order to evaluate the orders of magnitude for $\bar{E}_d$ and $\bar{N}_d$ we assumed that the concept of statistical collision cascade volume may be applied within the MeV energy range. Referring to the well known cascade model [6] we have further assumed that about 20% of the deposited energy is contained within a fractional volume V_f represented as a rotational ellipsoid with half axes corresponding to the longitudinal (σ_x) and transverse (σ_y) stragglings of the appropriate distribution. The correlation factors V_r relating the dimensions of the individual and statistical cascades appear to be energy independent for $M_2/M_1<1$ up to 0.1 MeV [7]. The lower limit for the $\bar{E}_d$ values was therefore estimated using V_r values given in reference [7]. According to the binary collision theory, the number of displaced atoms per ion may be estimated from the modified Kinchin-Pease formula [8]:

$N_{KP}=0.84E_v/2E_D$ where E_D is the displacement energy. Table I shows the N_{KP} values calculated using E_D=15 eV. Assuming that the defect creation rate $N=N_{KP}$ we calculated the approximate $\bar{E}_d$ and $\bar{N}_d$ values shown in Table I. We note that the $\bar{E}_d$ values used in this work are close to 10^{-4} - 10^{-5} eV/atom, an order of magnitude corresponding to the implantation of 30 keV He^+ or 300 keV O^+ions [6]. The maximum $\bar{N}_d$ value (5×10^{-6} displ./atom) is about 3 orders of magnitude lower than the average defect density required for the non-linear effects to become observable [6]. We also note however that for 1.25 MeV Si and 4.8 MeV Er the ratios: $\bar{E}_d(Er)/\bar{E}_d(Si)$ and $\bar{N}_d(Er)/\bar{N}_d(Si)$ are higher than 2. (Within the confines of the assumptions made these ratios are expected to be insensitive to the value of V_r). Given the low probability of the non-linear phenomena occuring, the type and distribution of crystalline defects in the "as implanted" state is expected to result primarly from the convolution of temperature dependent processes of recombination and clustering of point defects, as well as from the subsequent formation of extended defects such as stacking faults, twins and dislocations. The recently reported damage accumulation model [5] takes into account several temperature dependent mechanisms of interaction between the primary defects occuring during the implantation process. We refer phenomenologicaly to model [5] in an attempt to correlate the kinetics of point defects

interaction with the observed morphology of the high energy implanted Si. According to model [5], the probabilities of the Frenkel pairs forming stable clusters or recombining via intra-cascade interaction are expected to remain approximately constant within the temperature range $77K<T_i<RT$, whereas the probability of inter-cascade recombination is expected to increases considerably with increasing temperature [5]. The process is thermally activated: primary defects diffuse away from the cascade where they have originated and subsequently recombine with defects originating from different cascades. Assuming that the damage accumulation rate observed at 77K: $dN(77K)/dD=1$, the normalized rate $k=(dN(RT)/dD)/(dN(77K)/dD)$ (measured at an appropriate dose range) represents the fraction of the primary defects escaping recombination and forming stable complexes, thus contributing to the observed damage accumulation at RT. Consequently $(1-k)$ represents the fraction of primary defects recombining during the RT implantation process. Within the confines of the assumptions made the recombination rate $(1-k)N$ and the clustering rate kN are proportional to the defect creation rate N, so that the corresponding kinetics might be seen as first order reactions A+B=AB between randomly distributed partners A and B. However, if the concept of collision cascade applies to high energy implantation, primary defects will not be distributed at random and spatial correlation

effects might be expected to influence the interaction processes.

Assuming that the observed RBS-channeling yield Y is proportional to the number of displaced atoms, the normalized damage accumulation rates k were measured for the ion dose D range corresponding to a linear increase in dY(D)/dD. The experimentaly determined values of the fraction (1-k) are shown in Table I. We note that the average recombination rate decreases with increasing $\bar{N}_d$. Assuming that about 20% of interactions between the primary defects, leading to recombination or to clustering, occur within the fractional volume V_f, we calculated the average "recombination rate density" $\bar{R}_d$ and "clustering rate density" $\bar{C}_d$ for 1.25 MeV Si and 4.8 MeV Er ions, defined respectively as a number of recombining or clustering Frenkel pairs per ion and per unit volume (or per atom). The results shown in Table I indicate that an increase by a factor of 2 in the average defect density $\bar{N}_d$ results in an increase by a factor of 2 in the recombination rate density $\bar{R}_d$ and an increase by a factor of almost 5 in the clustering rate density $\bar{C}_d$. Since in the vicinity of RT the interaction between primary defects is expected to be dominated by the thermaly activated inter-cascade recombination process [5], one would expect the recombination and clustering rates as well as the corresponding rate densities to be controlled by the target

temperature rather than by ion species. The fact that at RT the recombination and clustering rates as well as the corresponding $\bar{R}_d$ and $\bar{C}_d$ values do depend on the ion species used, clearly suggests that the nucleation of stable defect clusters during high energy implantation is related to the primary defect density.

MORPHOLOGY OF THE IMPLANTED SYSTEM

- Liquid nitrogen implants.

The RBS/channeling spectra measured along the <100> axis and corresponding to the samples implanted at 77K are shown in Fig.2. The spectra are similar in shape: the backscattering yield increases monotonicaly with depth and reaches a maximum in the vicinity of the end of range (EOR), displaying a behaviour similar to the depth dependence of the dE_v/dx stopping power. The previously published XTEM data for LN temperature implantation of 1.25 MeV Si^+ ions [4] have shown that implantation results in the creation of a mixed phase in which discrete amorphous regions are present within the crystalline matrix. The density of the amorphous clusters increases with increasing depth and reaches a maximum value in the vicinity of the EOR. However, the average size of the isolated clusters (3-5 nm) is depth independent. The fact that cluster size is depth independent strongly suggests that it is determined

primarily by the kinetics of cluster growth during implantation at 77K. The isolated clusters produced at 77K are stable at RT and anneal out at temperatures close to 300°C, reducing the channeling yield within the surface region (SR) to nearly a virgin level, while the more complex EOR damage remains stable at this temperature [4].

Careful analysis of the variable energy RBS/channeling data for the 1 MeV O^+ implanted Si indicate that the observed dechanneling rate may also be attributed to complexes of point defects [9]. The concentration of displaced atoms within the surface layer was shown to be close to $1x10^{18}/cm^2$ for the oxygen dose of $3x10^{14}/cm^2$, a figure consistent with the estimation based on the N_{KP} value shown in Table I.

- Room temperature (RT) implantation.

The RBS/channeling spectra corresponding to the RT implantation are shown in Fig.3. In the case of 1.25 MeV Si^+ the RBS/channeling yield corresponding to the SR saturates at a relatively low level. The results of the XTEM analysis published earlier [10] indicated that although extended defects are present in a narrow region just ahead of the EOR damage, their nucleation and growth are suppressed within the SR and no amorphous clusters are present ahead of the EOR. Consequently, the SR damage detected by RBS/channeling

analysis is believed to consist of small isolated defect complexes. This is consistent with the earlier reported data on isothermal annealing experiments [11] showing that the damage present in the surface layer anneals out at 200°C. The 200°C annealing stage has been associated with the di-vacancy defect [12]. Although the presence of higher order vacancy complexes cannot be excluded, the di-vacancy is thought to be the predominent defect type within the SR of the 1.25 MeV Si implanted samples. The fact that no amorphous clusters have been observed after RT implantation within the SR indicates that most of the isolated amorphous nuclei formed during the Si implantation and able to grow during implantation at 77K, are unstable at RT. Such behaviour would be consistent with a principle common to all changes in condensed systems: when a new phase is produced within the host lattice, its formation is controlled by the existence of a temperature dependent critical size having an equal probability of shrinking or growing. Below the critical size the embryos of the new phase are unstable [13]. However, the situation appears to be more complicated in the vicinity of the EOR where the damage morphology is believed to result from the competition between the instability of isolated nuclei, and the high $\bar{N}_d$ related interaction between spatially correlated nuclei, leading to the formation of defect complexes large enough to remain stable or to grow during the RT implantation.

In an attempt to answer the question of whether or not the thermal stability of cluster nuclei is related to the $\bar{N}_d$ value, we implanted 4.8 MeV Er^+ ions at RT. Fig.3 clearly shows that for the RT Er implants the backscattering yield increases with increasing ion dose within the entire investigated depth. For the 4.8 MeV Er dose of $2\times10^{13}/cm^2$, a 1-hour thermal annealing at 200°C, leads to a 60% decrease in backscattering yield throughout the whole investigated depth (results not shown), indicating that di-vacancy may be the dominating defect species. However, the presence of a small amount of amorphous clusters cannot be excluded. Further investigation is necessary to verify this point.

- Implantation of 4.8 MeV Er at $RT<T_i<200°C$.

At $T_i>100°C$ the inter-cascade recombination rate reaches saturation while the intra-cascade annihilation rate, as well as the mobility of vacancy complexes, increase significantly [5]. Assuming the activation energy for di-vacancy migration to be 0.18 eV [14], the corresponding diffusion length at 180°C is of the order of tens of μm. Consequently, the probability of the point defects forming stable clusters is expected to decrease progressively with increasing T_i. Fig.4 shows the RBS/channeling spectra corresponding to a dose of $6\times10^{13}/cm^2$ of 4.8 MeV Er^+ implanted at $RT<T_i<200°C$. We note that for $RT<T_i<180°C$ the backscattering yield remains essentially unchanged in the

vicinity of the surface, whereas the EOR damage accumulation rate decreases significantly with increasing T_i. The observed decrease in the EOR damage strongly suggests that the defect complexes nucleated within the EOR region (and stable at RT) are unstable during implantation at 180°C. An increase in T_i from 180°C to 200°C leads to a further significant decrease in damage accumulation rate (see Fig.4). The result is consistent with the 200°C annealing results mentioned above. The fact that the decrease in RBS/channeling yield occurs throughout the entire investigated depth range is attributed to a decrease in thermal stability of vacancy complexes [10]. For T_i=200°C preliminary results of XTEM analysis indicate the presence of small defects throughout the whole analysed depth. Although the defects have not been identified so far, they are believed to be amorphous clusters. We note that elongated interstitial clusters have been observed using HREM in Si single crystal implanted with 150 keV Si^+ ions at 200°C [15]. No dislocation loops have been observed. Finally, no measurable damage was found for T_i>300°C for the dose used in this experiment.

- Interaction of 4.8 MeV Er induced defects with pre-existing damage.

It has been reported earlier that at RT an interaction between high energy Si ions with the pre-existing damage may result in either a reduction in or an accumulation of the damage, depending on the morphology of the pre-existing defect structure [10]. In order to obtain some insight into the process of defect interaction with the pre-existing damage within the technologically relevant temperature range $RT<T_i<200°C$ we have implanted $6x10^{13}/cm^2$ of 4.8 MeV Er^+ ions at $T_i=200°C$ into a sample pre-implanted with $4.5x10^{13}/cm^2$, 4.8 MeV Er^+ at RT. The corresponding RBS/channeling spectra are shown in Fig.5. The re-implantation at 200°C leads to no observable increase in the backscattering yield in the vicinity of the EOR. However, a significant increase in the RBS/channeling yield occurs in the surface region: within a depth of about 1 μm the channeling yield reaches a level higher than the arithmetic sum of the spectra corresponding respectively to the RT and 200°C implantations. The observed increase in channeling yield during re-implantation at 200°C is attributed to the ability of the pre-existing defects produced at RT to act as sinks for the primary defects. The results of the trapping process are expected to depend on the morphology of the pre-existing damage and thermal stability of the trapping centers. However, further investigation is necessary in order to explain the behaviour

of the EOR damage during the re-implantation process.

SUMMARY AND CONCLUSION.

1. We have provided experimental evidence to show that, although the $\bar{N}_d$ values used in this work are considerably lower than those required for the non-linear effects to become observable, nucleation of defect clusters during high energy implantation is related to the density of primary defects and resulting proximity effects.

2. We have shown that the morphology of high energy implanted Si in the "as implanted" state is related to the thermal stability of cluster nuclei and their ability to grow during the implantation process. Growth of a defect cluster is belived to occur via random addition of primary defects transported to the growing nuclei by diffusion.

3. We have also shown that for the technologically relevant implantation temperature range $RT<T_i<200°C$, the morphology of the implanted system is related to the pre-existing damage which may act as trapping sites for primary defects. The trapping process may lead to further damage accumulation within the surface layer at T as high as 200°C. The interaction of simple defects with the pre-existing damage may have direct technological implications as the high energy implantation could modify the morphology of the system within the active zone of the device.

REFERENCES

[1] A.N.SAXENA and D.PRAMANIK

Material Science and Engineering B2, 1 (1989)

[2] J.P.BIERSACK and L.G.HAGGMARK

Nucl.Instrum.Methods, 174, 257 (1980).

[3] D.A.THOMPSON

Rad.Effects 56, 105 (1981).

[4] O.W.HOLLAND, C.W.WHITE, M.K.EL-GHOR and J.D.BUDAI

J.Appl.Phys. 68, 2081 (1990).

[5] N.HECKING and E.H.TE KAAT

Applied Surface Science 43, 87 (1989).

[6] D.A.THOMPSON and R.S.WALKER

Nucl.Instrum.Methods. 132, 281 (1976).

[7] R.S.WALKER and D.A.THOMPSON

Rad.Effects 37, 113 (1978).

[8] P.SIGMUND

Appl.Phys.Lett.14,114 (1969).

[9] A.GROB, J.J.GROB, P.THEVENIN and P.SIFFERT

Mat.Res.Symp.Proc. Vol.147, 197 (1989).

[10]O.W.HOLLAND, M.K.EL-GHOR and C.W.WHITE

J.Mater.Res. 5, 352 (1990).

[11]O.W.HOLLAND, M.K.EL-GHOR and C.W.WHITE

Appl.Phys.Lett.53, 1282 (1988).

[12]F.L.VOOK and H.J.STEIN

Radiat.Eff.2,23 (1969).

[13]J.BURKE

The Kinetics of Phase Transformations in Metals

Pergamon, London (1965).

[14]J.NAKATA, M.TAKAHASHI and K.KAJIYAMA

Jap.J.Appl.Phys. 20, 2211 (1981).

[15]C.PRUNIER, E.LIGEON, A.BOURRET, A.C.CHAMI

and J.C.OBERLIN

Nucl.Instr. and Methods in Physics Research

B17, 227 (1986)

TABLE I

ION	M_2/M_1	E (MeV)	E_ν (keV)	R_p(dam.) (μm)	N_{KP}	$\bar{E}_d$ (eV/atom)	$\bar{N}_d$ (FP/atom)	1-k	$\bar{R}_d$ (rec./at.)	$\bar{C}_d$ (cl./at.)	
O^+	1.76	1.	92	1.3	2240	6.9×10^{-5}	1.9×10^{-6}	0.98			*
Si^+	1.	1.25	163	1.3	4550	7.8×10^{-5}	2.1×10^{-6}	0.83	1.7×10^{-6}	4.0×10^{-7}	*
Si^+	1.	2.	180	2.0	5040	4.0×10^{-5}	1.1×10^{-6}				**
Ni^+	0.48	6.	600	2.9	16800	2.3×10^{-5}	6.5×10^{-7}				**
Er^+	0.17	4.8	1392	1.1	38970	1.8×10^{-4}	5.1×10^{-6}	0.67	3.2×10^{-6}	1.9×10^{-6}	*

* ion used in this work;
** ion used in ref.(5).

FIGURE CAPTIONS

FIG.1: *Relative contribution of the elastic and inelastic energy losses for the ions used or quoted in this work.*

FIG.2: RBS/channeling spectra for the 77K implants (as implanted). Virgin (V) and random (R) spectra are shown for comparison:

A: 1 MeV O^+ ($3\times10^{14}/cm^2$),

B: 1.25 MeV Si^+ ($3\times10^{14}/cm^2$): as implanted (a) and annealed 300°C/30 min (b);

C: 4.8 MeV Er^+: $5\times10^{12}/cm^2$ (a), $1\times10^{13}/cm^2$ (b) and $2\times10^{13}/cm^2$ (c).

FIG.3: RBS/channeling spectra for RT implants (as implanted). Virgin (V) and random (R) spectra are shown for comparison:

A: 1 MeV O^+ ($2\times10^{16}/cm^2$),

B: 1.25 MeV Si^+ ($3\times10^{15}/cm^2$),

C: 4.8 MeV Er^+: $1\times10^{13}/cm^2$ (a), $4\times10^{13}/cm^2$ (b) and $6\times10^{13}/cm^2$ (c).

FIG.4: RBS/channeling spectra for 4.8 MeV Er^+ ($6\times10^{13}/cm^2$) implanted at RT (a), 180°C (b) and 200°C (c).

FIG.5: RBS/channeling spectra corresponding to the double implantation experiment (4.8 MeV Er^+):

a: RT, 4.5×10^{13} /cm^2,

b: 200°C, 6×10^{13} /cm^2,

c: double implantation:

RT (4.5×10^{13}/cm^2) + 200°C (6×10^{13}/cm^2),

d: sum of the spectra: (d) = (a) +(b)

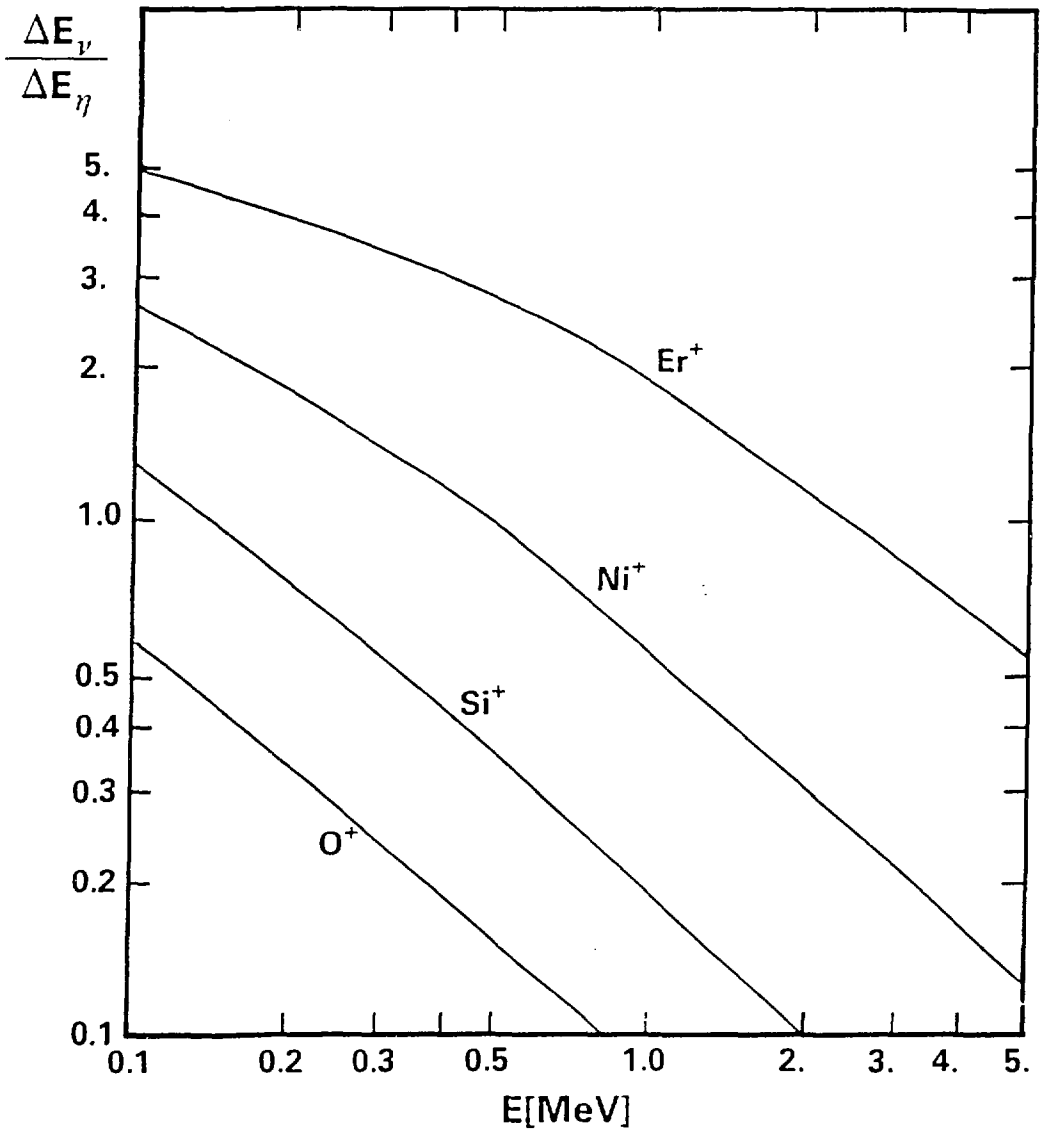
$\frac{\Delta E_\nu}{\Delta E_\eta}$
5.
4.
3.
2.
1.0
0.5
0.4
0.3
0.2
0.1
0.1
0.2
0.3
0.5
1.0
2.
3.
4.
5.
E[MeV]
Er^+
Ni^+
Si^+
O^+

FIG. 1

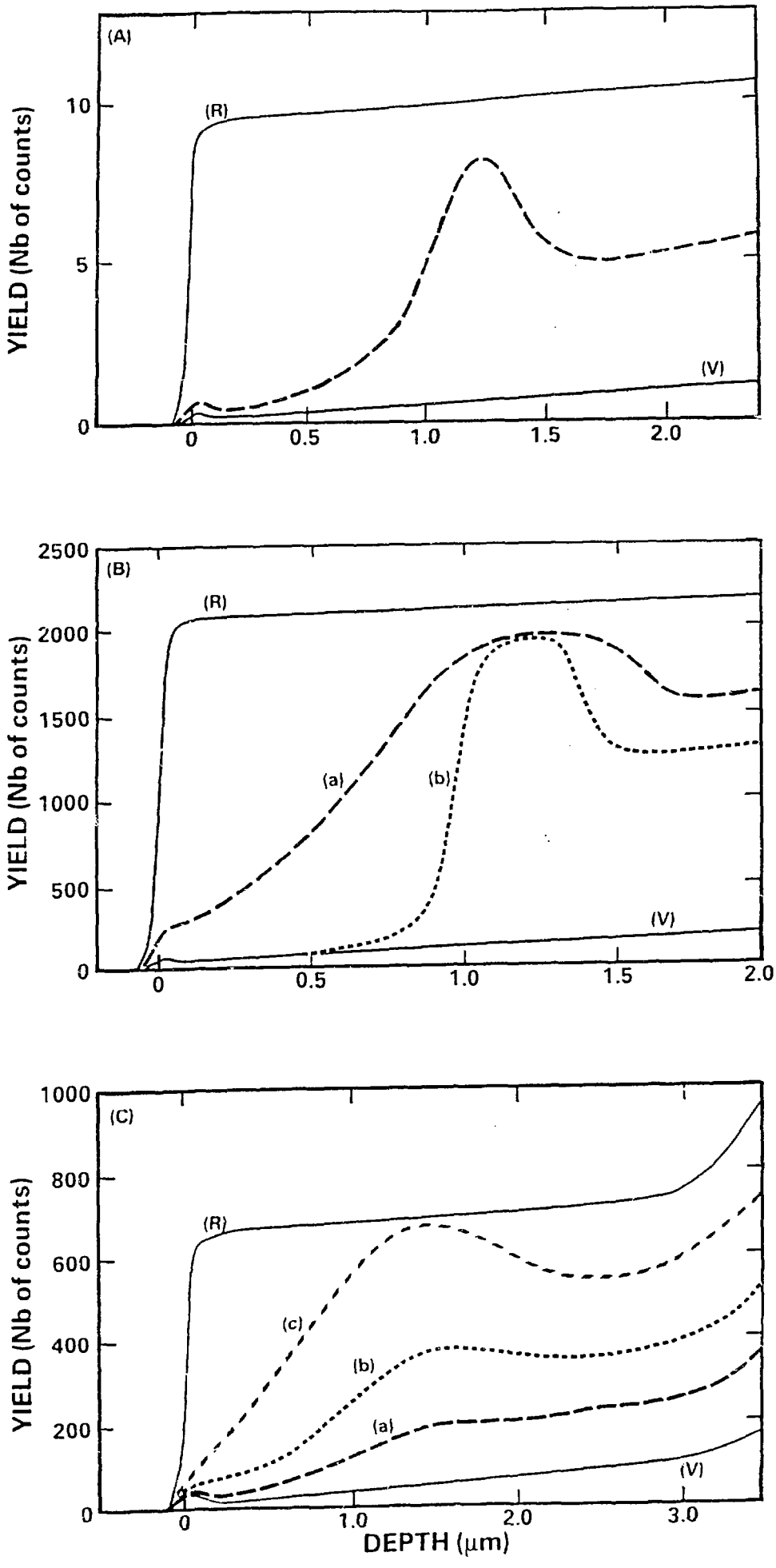
(A)
YIELD (Nb of counts)
10
5
0
(R)
(V)
0
0.5
1.0
1.5
2.0
(B)
2500
2000
1500
1000
500
0
(R)
(a)
(b)
(V)
(C)
1000
800
600
400
200
(R)
(c)
(b)
(a)
(V)
3.0
DEPTH (μm)

FIG.2

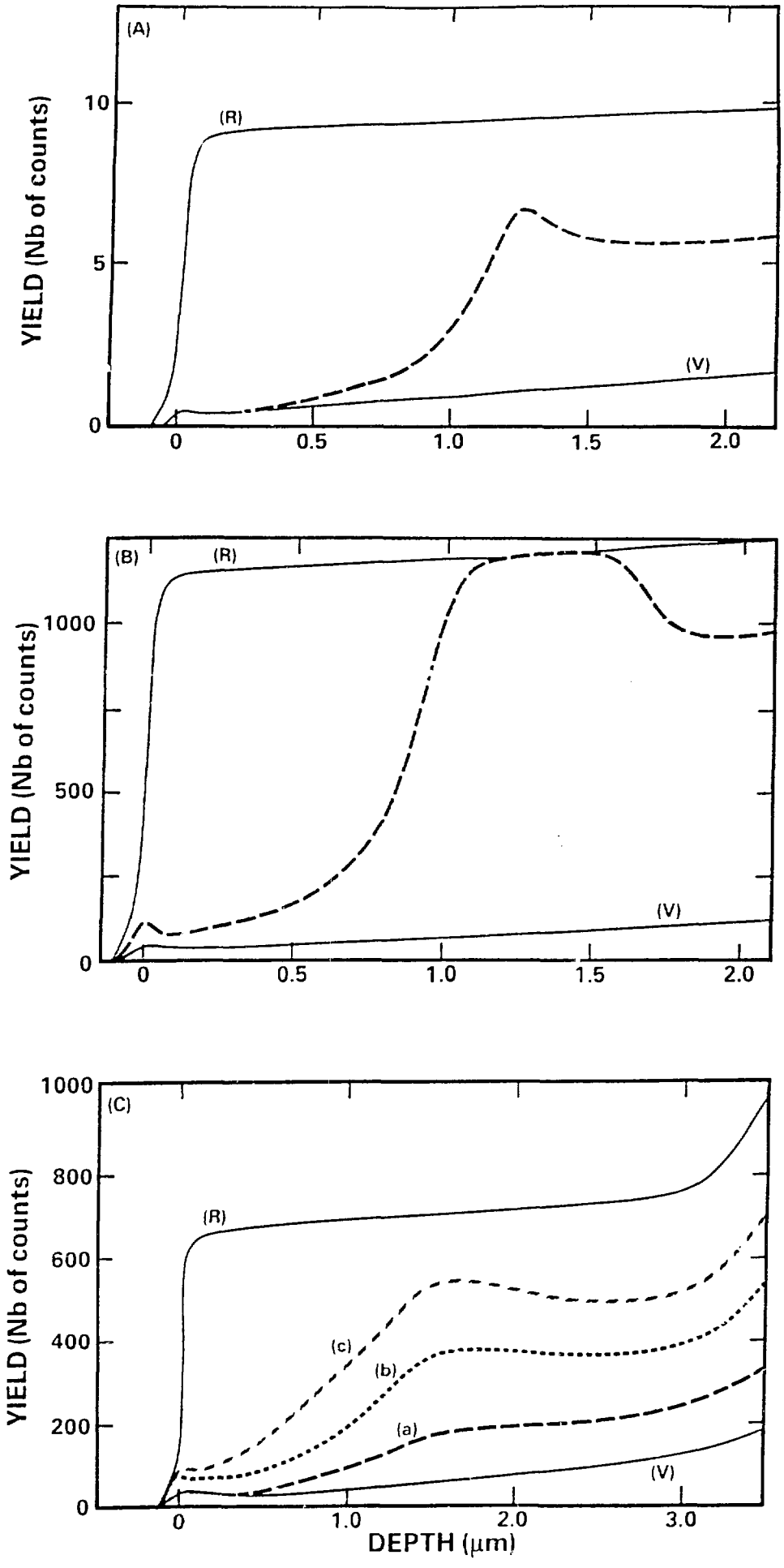
(A)
YIELD (Nb of counts)
10
5
0
(R)
(V)
0
0.5
1.0
1.5
2.0
(B)
(R)
YIELD (Nb of counts)
1000
500
0
(V)
0
0.5
1.0
1.5
2.0
(C)
YIELD (Nb of counts)
1000
800
600
400
200
0
(R)
(c)
(b)
(a)
(V)
0
1.0
2.0
3.0
DEPTH (μm)

FIG.3

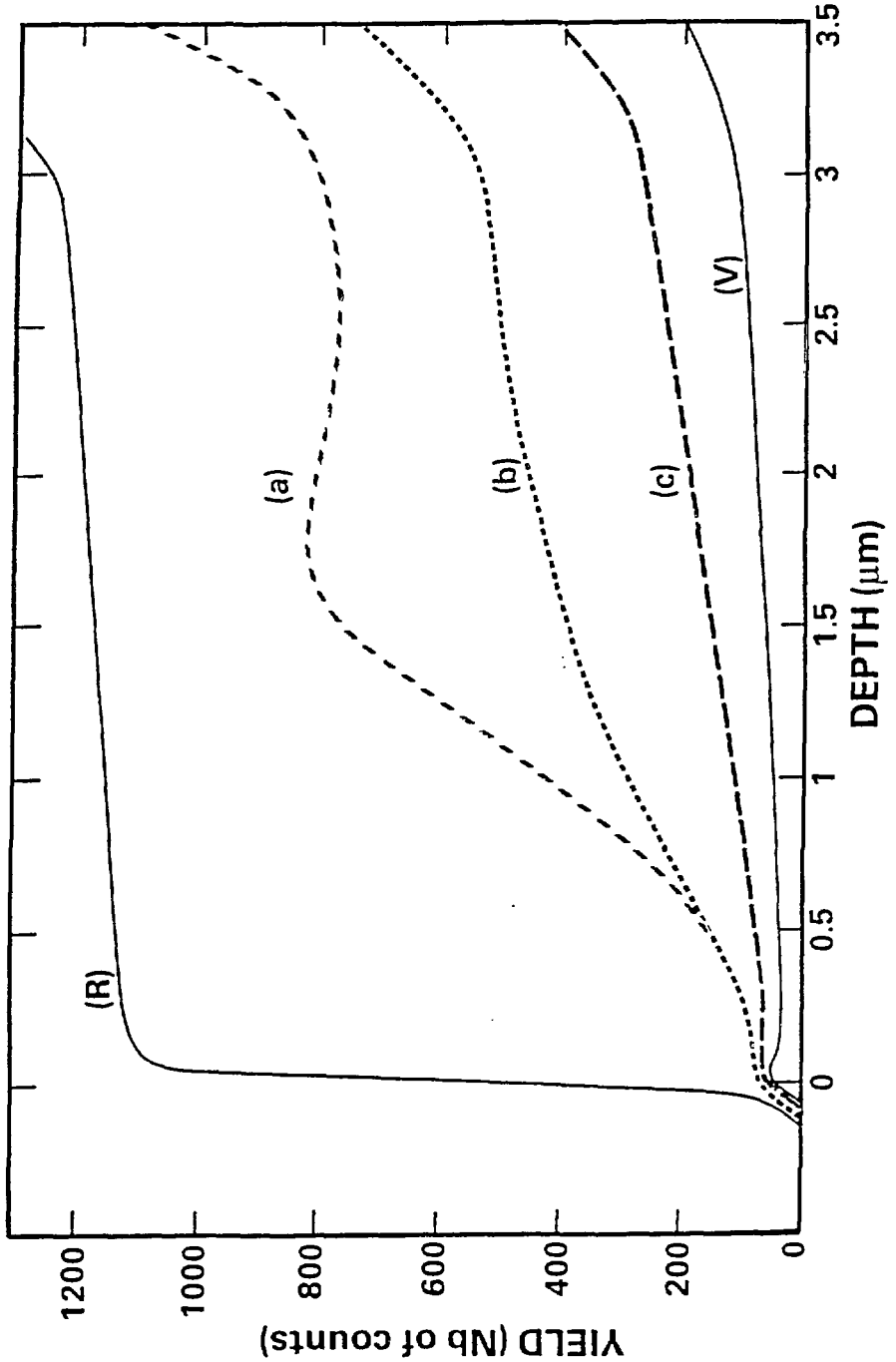
YIELD (Nb of counts)
1200
1000
800
600
400
200
0
DEPTH (μm)
0
0.5
1
1.5
2
2.5
3
3.5
(R)
(a)
(b)
(c)
(V)

FIG.4

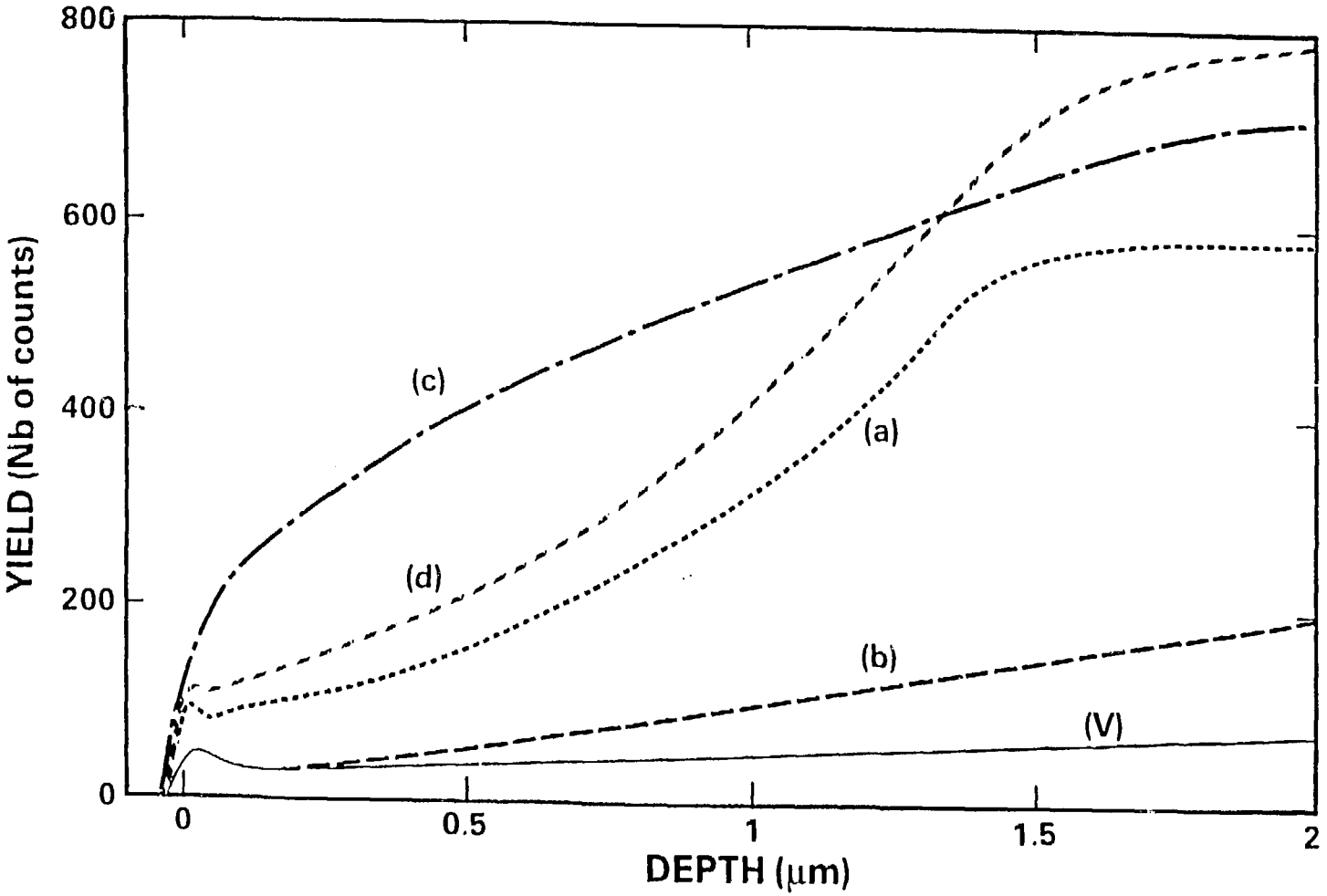
800
600
400
200
0
YIELD (Nb of counts)
0
0.5
1
1.5
2
DEPTH (μm)
(c)
(d)
(a)
(b)
(V)